AIAA 2005-4760

35th AIAA Fluid Dynamics Conference and Exhibit
Toronto, Ontario

# A Biologically Inspired Computational Study of Flow Past Tandem Flapping Foils

I. Akhtar* and R. Mittal§

*Department of Mechanical & Aerospace Engineering*
*The George Washington University, Washington DC –20052*

**Numerical simulations have been used to analyze the effect that vortices, shed from one flapping foil, have on the thrust of another flapping foil placed directly downstream. The simulations attempt to model the dorsal-tail fin interaction observed in a live bluegill sunfish by Drucker & Lauder[4-6] using Particle Image Velocimetry (PIV). The simulations have been carried out using a Cartesian grid method that allows us to simulate flows with complex moving boundaries on stationary Cartesian grids. The simulations indicate that vortex shedding from the upstream dorsal fin is indeed capable of increasing the thrust of the tail fin significantly. However, this thrust augmentation is found to be quite sensitive to the phase relationship between the two flapping fins. The numerical simulations allows us to examine the underlying physical mechanism for this thrust augmentation.**

## I. Introduction

Many engineered systems tend to emulate what is observed in nature. Engineers are increasingly looking for inspiration from nature and there is a great interest in making miniature machines that can mimic those found in nature. Researchers[1] have built a micro-aerial vehicle of the size of a housefly. Similarly, several physico-mechanical designs evolved in fish are currently inspiring robotic devices for propulsion and maneuvering purposes in underwater vehicles.[2] One engineered system that could substantially benefit from biological inspiration is the autonomous underwater vehicle (AUV). As research and use of AUVs is expanding[3], there is increased demand for improved efficiency and performance to allow for longer and more complex missions.

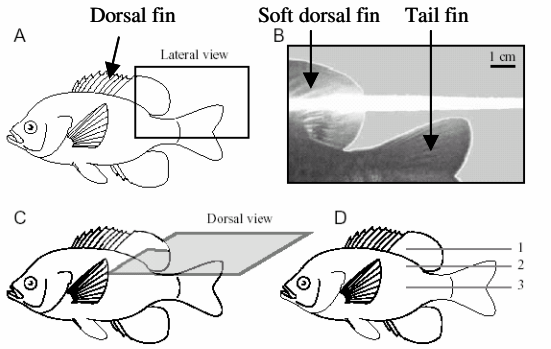


**Figure 1. Experiment of Drucker and Lauder 2001. (Drucker and Lauder, 2001)**

Recently Drucker and Lauder[4-6] have performed several experiments with bluegill sunfish (see figure 1). In their experiments, they have used the technique of Digital Particle Image Velocimetry (DPIV) in order to visualize the wake structures and to calculate locomotion forces. In one of their experiments[6], they have studied the effect of the presence of a soft dorsal fin on the thrust and efficiency of the tail fin, and this experiment is of major significance to the current study. Moreover, they have also examined the hydrodynamic impact of the vortices produced by the soft dorsal fin on the tail fin and the vortices generated by the tail fin itself. Figure 2 video images of the two fins within a frontal plane laser sheet (Figure 1 D, position 2) over the course of one complete stroke cycle during steady swimming. In their results, they have hypothesized that the presence of dorsal fin upstream of the tail fin augments thrust and the overall propulsive efficiency.

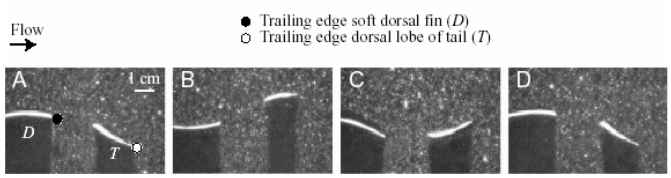


**Figure 2. Experimental result of Drucker and Lauder (Drucker and Lauder, 2001)**

* **Current Affiliation: Graduate Research Assistant**
**Department of Engineering Science and Mechanics, MC 0219**
**Virginia Tech, Blacksburg, VA 24060**
**Student Member**
§ **Associate Professor, 801 22nd St, Suite T729, NW**
**Washington DC 20052**
**Senior Member**

In this paper, the main objective is to examine this hypothesis by studying the interaction of the soft dorsal fin with the tail fin through numerical simulations. In order to investigate this effect, it is useful to first study the situation where the soft dorsal fin is not present upstream of the tail. This could be attempted in experiments by ablating the soft dorsal fin from a fish, but it would be difficult to interpret the behavior/gait of the fish in this state. However, in a computational model, it is possible to simulate the flow past a tail fin with no upstream dorsal fin and study its thrust and efficiency. Subsequent simulations of the tail fin with an upstream soft dorsal fin allow us to clearly assess the effect of the soft dorsal fin on the tail fin performance.

## II. Computational Modeling

Combined pitch and heave is the primary fin motion through which birds, insects and fish produce the thrust and lift required for motion. The experiment of Drucker and Lauder[6] indicates that the dorsal and tail fin motion of the bluegill sunfish can also be well approximated as a combined pitch and heave motion. A foil in a steady forward motion and a combination of harmonic heaving and pitching motion produces thrust through the formation of a flow downstream from the trailing edge, which, when averaged over one period of oscillation, has the form of a jet. Pitch and heave motions are mathematically modeled as follows assuming that the pitch leads heave by 90° as shown in figure 3.

$$\textit{Pitch}: \quad \theta(t) = \theta_{\max} \cos(\omega t) \tag{1}$$

$$\textit{Heave}: \quad y(t) = y_0 + A\sin(\omega t) \tag{2}$$

Table 1. Fin non-dimensional parameters

| Parameter | Soft Dorsal Fin ($d$) | Tail Fin ($t$) |
|---|---|---|
| Amplitude to chord ratio ($A/c$) | 0.32 | 0.56 |
| Thickness ratio ($t/c$) | 1/12 | 1/8 |
| Max Pitch angle ($\theta_{max}$) | ~ 20° | ~ 30° |
| Phase angle between heave and pitch ($\psi$) | 90° | 90° |
| Reynolds number (Re = $U_\infty c/\nu$) | 630 | 600 |
| Strouhal Number (St = $fL/U_\infty$) | 0.19 | 0.28 |
| Chord ratio ($c_d / c_t$) | 1.06 | |
| Mean Distance between fins ( $l/c_t$ ) | 0.99 | |
| Phase difference ($\phi$) between fins | 108° | |

The non dimensional fin parameters for single and tandem foil configurations are defined in Table 1. Examination of the experimental data indicates that the dorsal fin leads tail fin by a 108° phase difference. For this specific case, the soft dorsal and the tail fins can therefore be modeled as two foils in tandem (see figure 4) undergoing pitch and heave motion with the same phase difference between them. In the numerical simulations, these foils are modeled as rounded plates undergoing this motion. There are obvious limitations of the current computational model in terms of the simplifications that have been assumed with regarding the fin geometry and kinematics. However, despite all these limitations of the computational modeling, it is expected that the results of the analysis would lead to some useful insights on the dorsal-tail fin interaction. The Reynolds number (Re) during the experiment is about 5000 which requires a high resolution grid for the numerical simulations. Due to this the numerical simulations were carried out at a Re of 600 to limit the grid requirements and obtain grid independent results. It should be pointed out that the Strouhal number (St), which is a key parameter for the flapping foils, is matched between the simulations and experiment.

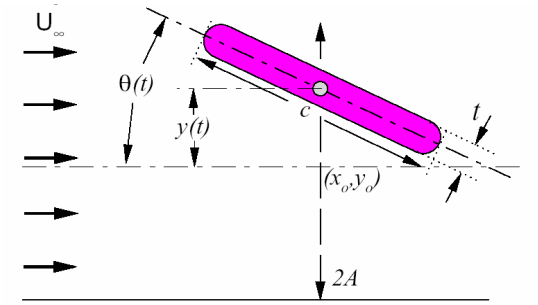


**Figure 3. Schematic diagram of a fin moving up**

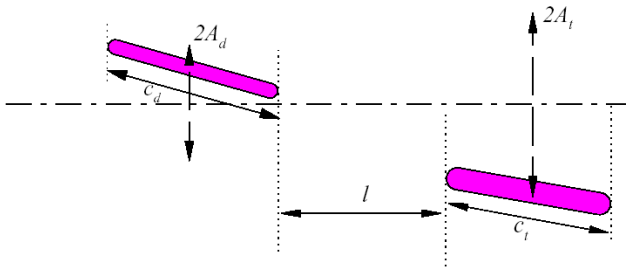


**Figure 4. Schematic diagram of soft dorsal and tail fin.**

## III. Numerical Method

A Cartesian grid solver by Udaykumar et al.[7] and Ye et al.[8] is employed in these simulations. The advantage of this method is that the complexity and cost of generating a body-conformal mesh at each time-step is eliminated, thereby easing the resources required to perform such simulations.

The fractional step scheme is used for advancing the solution in time. The Navier-Stokes equations are discretized on a Cartesian mesh using a cell-centered collocated (non-staggered) arrangement of the primitive variables $(\vec{u}, p)$. The integral forms of the non-dimensionalized governing equations are used as the starting point:

$$\oint \vec{u}.\vec{n}dS = 0 \tag{3}$$

$$St\frac{\partial}{\partial t}\oint \vec{u}dV + \oint \vec{u}(\vec{u}.\vec{n})dS = -\oint p\vec{n}dS + \frac{1}{\mathrm{Re}}\oint \nabla\vec{u}.ndS \tag{4}$$

where $\vec{u}$ is non dimensional velocity vector, $p$ is pressure and $\boldsymbol{n}$ is a unit vector normal the face of the control volume. The above equations are to be solved with $\vec{u}(\vec{x},t) = \vec{u}_\partial(\vec{x},t)$ on the boundary of the flow domain where $\vec{u}_\partial(\vec{x},t)$ is the prescribed boundary velocity, including that at the immersed boundary. A non-uniform Cartesian grid is employed to carry out the analysis as shown in figure 5.

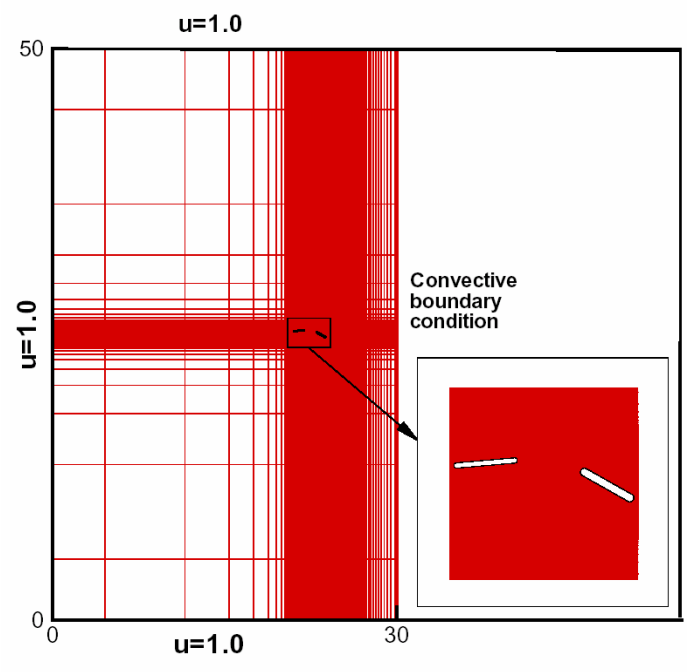


**Figure 5. Non-uniform grid.**

## IV. Results

Numerical simulations have been carried out in order to understand the effect of the soft dorsal fin on the tail fin. With the help of computational modeling, the results of two fin simulations are compared one to one with a single fin model of the tail fin by just removing the upstream soft dorsal fin. Thus there are two distinct cases:

1) Configuration I : Tail fin only.
2) Configuration II : Soft dorsal fin and tail fin.

### A. Performance of an Oscillating foil

In the analysis of the performance of an oscillation foil, the key performance factors are thrust and efficiency.[9,10] Considering the rounded plate, as shown in figure 3, the fin is subjected to time varying forces *T(t)*, *S(t)* in the x- (forward) and y- (transverse, or lift) directions, respectively; and a torque *M(t)* about its center. The forces and moments on the foils are computed by numerically integrating the pressure and shear stresses on the surfaces of the foils.

For any general function *f(t)*, the average over *N* cycles is defined as

$$\langle f \rangle = \frac{1}{N\tau} \int_0^{N\tau} f(t)dt \tag{5}$$

Thus the average thrust coefficient $c_T$ is defined as

$$c_T = \frac{\langle T \rangle}{\frac{1}{2}\rho U^2 c} \tag{6}$$

where $\rho$ denotes the fluid density and $c$ is the chord length of the tail fin. Furthermore, the propulsive efficiency, $\eta_p$, is defined[10] as the ratio of useful power to input power (*P*).

$$\eta_p = \frac{\langle TU \rangle}{P} = \frac{\langle T \rangle U}{P} \tag{7}$$

where

$$P = \left\langle S.\dot{y} \right\rangle + \left\langle M.\dot{\theta} \right\rangle \tag{8}$$

**B. Simulation Results**

Grid and domain independence studies are critical in order to verify the accuracy of the computation results. Extensive grid and domain independence studies have been carried out in order to ensure that the results are not sensitive to these factors. The grid used in the current simulation is 520 x 240 with the domain size of 30 x 50 as shown in figure 5. The grid size was increased to 700 x 430 and it is observed that the percentage difference for the thrust and lift forces is less than 5% which clearly indicates that the flow in the vicinity of the foils is virtually grid independent. Similarly, the domain size was increased to 40 x 60 with grid size of 577 x 262. The slight increase in the grid size is to maintain comparable grid spacing in the two grids. It is observed that the percentage difference for the thrust and lift forces is less than 3% verifying the domain independence for this study. Details of the grid and domain independence study are given in Akhtar[11] (2003).

In configuration I, Figure 6 (A-L) shows vorticity contours during a half cycle of the tail fin in which the fin moves from the bottom-most position to the top-most position. The blue and red contours represent positive and negative vorticity, respectively. Figure 6 A shows the tail fin at the bottom of its cycle. As the fin moves up, the pitch angle also increases (6 B&C). The clockwise vortex is created on the top of the tail fin and is about to be detached (figure 6 D&E). In figure 6 F, the tail fin has reached the mean position and is at its maximum pitch angle of 30°. As it moves up further, the pitch angle starts decreasing as shown in figure 6 H. The counter clockwise vortex starts developing below the tail fin near TE. The tail fin peaks to its maximum amplitude where the pitch

**Table 2. Comparison of Configuration I & II.**

| Parameter | Configuration I Tail only | Configuration II 108° phase | %age increase |
|---|---|---|---|
| Thrust Coefficient ($C_T$) | 0.128 | 0.272 | 107 % |
| Efficiency ($\eta_P$) | 0.172 | 0.261 | 52 % |

angle becomes zero. These pictures depict half the cycle of the tail fin and the rest of the cycle can be obtained as an image of this across the axis of symmetry of the pitching motion. This completes one cycle of the tail fin in which we get a pair of vortices. In configuration II, vorticity contours are shown at the same instant as that of configuration I in order to have direct comparisons between the two cases. In figure 7 A, the vortex shedding is different from its corresponding counterpart. Similarly in figure 7 F, due to the presence of soft dorsal fin upstream of the tail fin, the vortex is formed below the tail fin at almost half its chord length and is significantly bigger. In figure 7 K, a complete vortex is formed at the TE of tail fin. In figure 7 K, the counter clockwise vortex is shed, and it is larger in size as compared to that of configuration I. These pictures also depict half of the cycle of the fins.

The thrust, side force and the moment coefficients are plotted against time for comparison of the two cases. Figure 8 shows various locations of the tail fin at different instants. In figure 9, heaving velocity and pitch angle are plotted for different positions of the tail fin at various instants. It is clear that when the fin is at the center position, its heave (vertical) velocity and pitch angle (-ve going up) are at peak values and are minimum at the extreme positions. Two complete cycles are plotted for the thrust coefficient against time in figure 10. Different positions of the tail fin are marked on the x–axis corresponding to the thrust at that location on the y-axis.

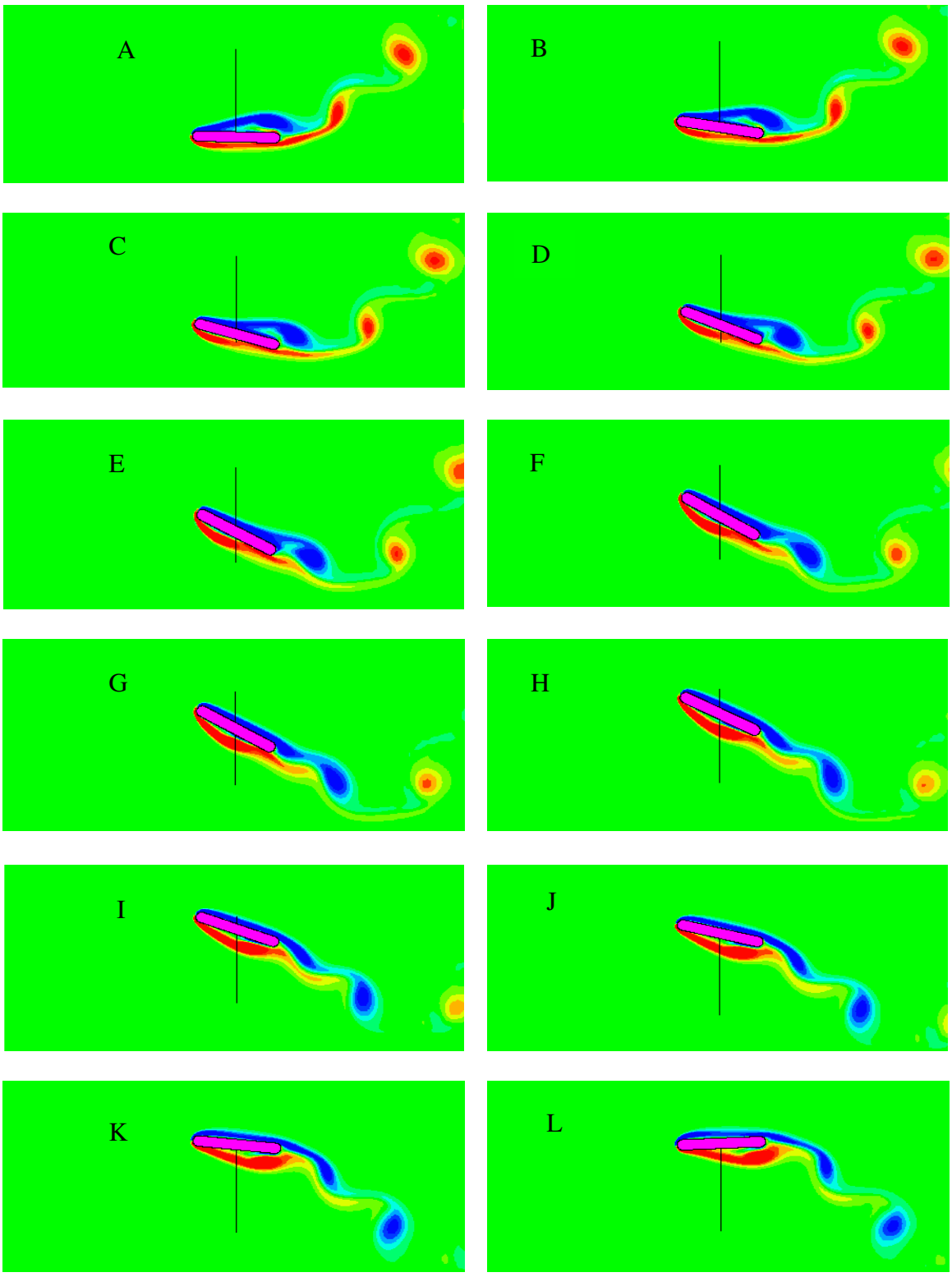


**Figure 6. Configuration I : Tail Fin Only case**

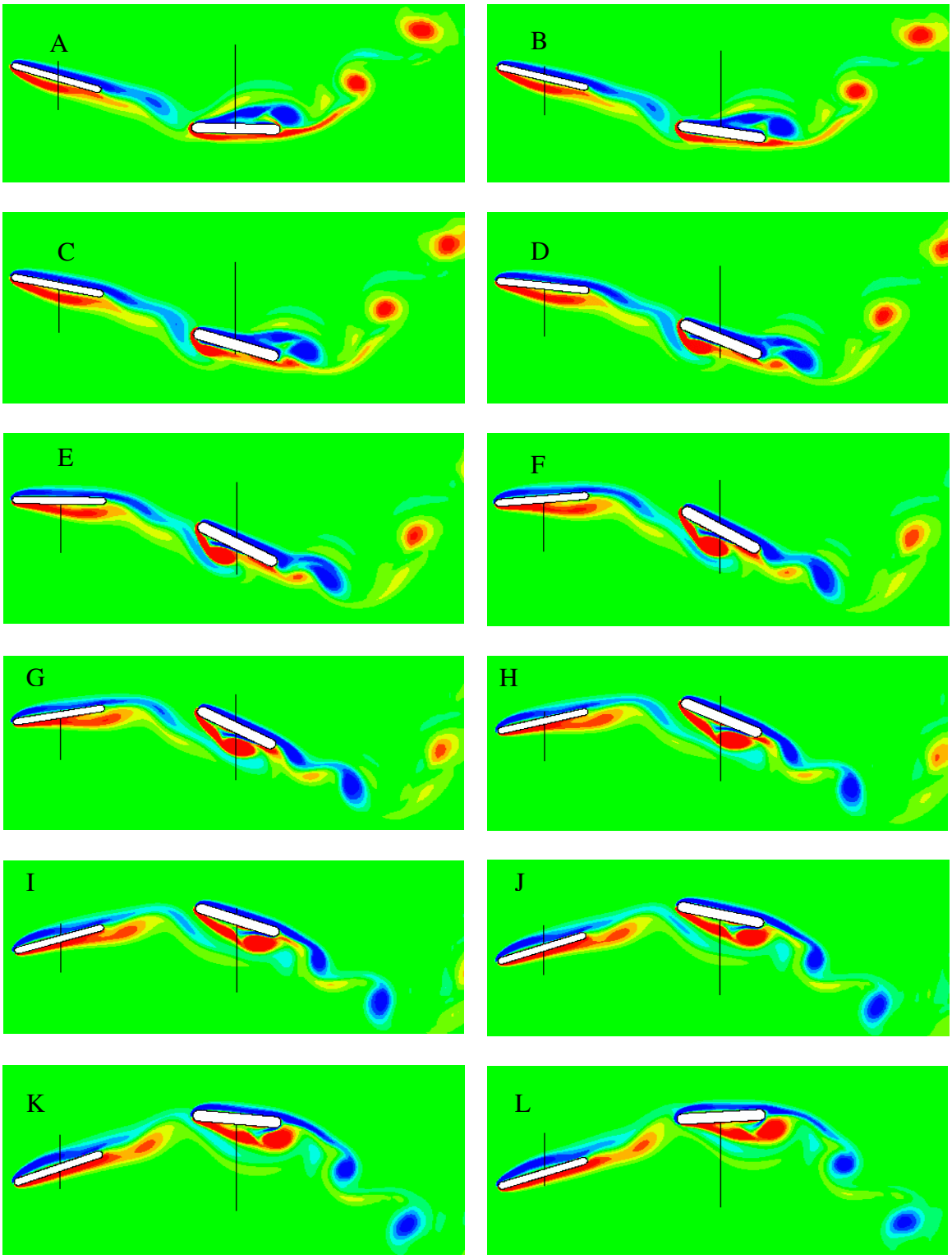


**Figure 7. Configuration II : Soft Dorsal Fin and Tail Fin**

It is observed that there is a significant increase in the thrust of the tail fin due to the presence of the soft dorsal fin, primarily during the phase when the foil accelerates towards its mean position. Similarly in figure 11, the side force is compared for the two cases. As expected, the side force is equal in magnitude but opposite in direction for the two halves of a complete cycle. The moment plot against time is shown in figure 12. The moment coefficient is also symmetric for the two halves of a complete cycle. The thrust and efficiency of the tail fin are calculated and are shown in Table-1 for each configuration.

The numerical simulations therefore clearly indicate that the presence of the upstream fin can greatly increase the thrust and efficiency of the tail fin. However, it is not sufficient to conclude, based on one set of simulations, that the upstream fin enhances the performance of the downstream fin. For the results of this study to be useful, it is required to:

1) Explain the physical mechanism(s) that is(are) responsible for this performance enhancement.
2) Determine what is/are the key factors that influence this enhancement.

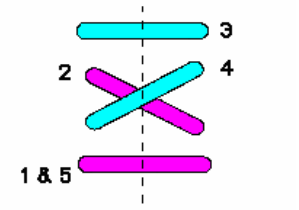


**Figure 8. Position of the tail fin at different instants.**
1&5-Bottom position,
2-Center position (moving up),
3-Top position,
4-Center position (moving down)

In order to investigate what factors actually affect the performance of the tail fin when there is a soft dorsal fin located upstream, the vorticity plots of the two configurations are placed side by side for a direct comparison.

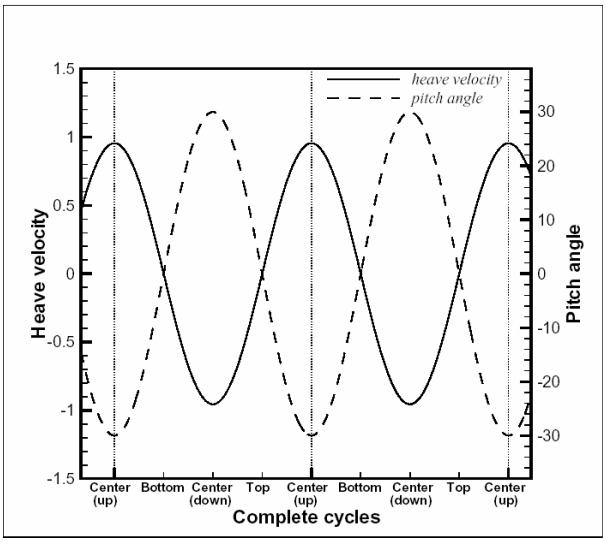


**Figure 9. Heave velocity and pitch angle vs time**

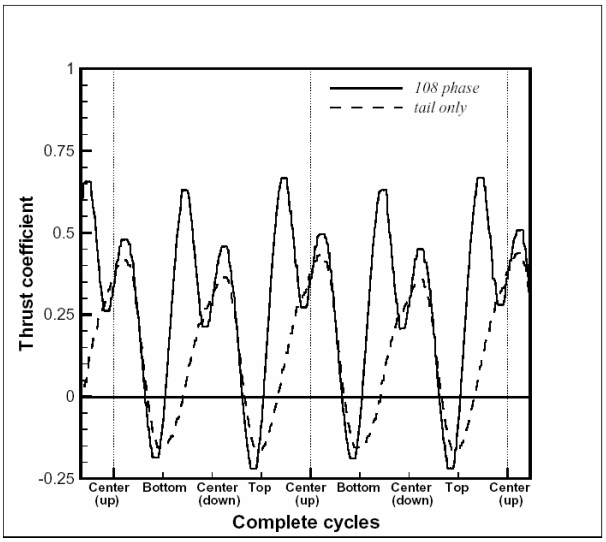


**Figure 10. Thrust coefficient comparison vs time**

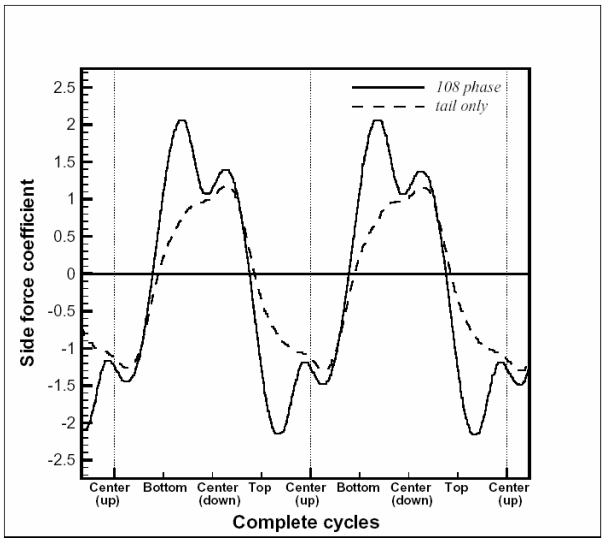


**Figure 11. Side force comparison vs time**

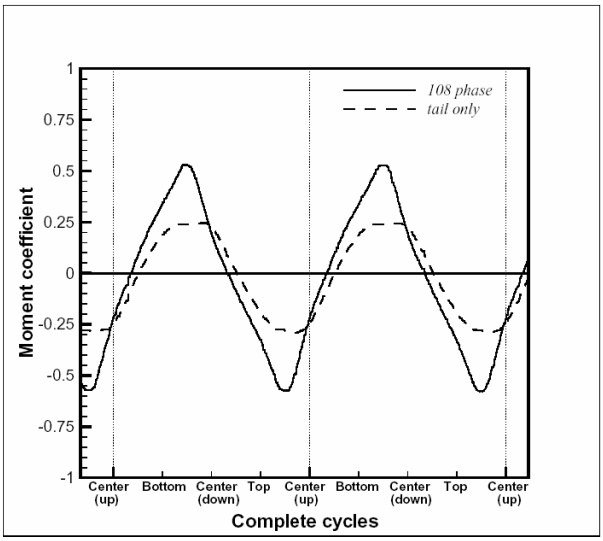


**Figure 12. Moment coefficient comparison vs time**

Moreover a zoom-in view is also shown in figure 13 along with the velocity vectors. The following observations are made regarding this comparison:

1) By observing the velocity vector upstream of the tail fin, it is seen that the effective angle of attack (AOA) of the flow of the tail fin for Configuration II is larger than that of Configuration I. This is defined as the effective AOA as seen by the tail fin. The increase in AOA in Configuration II is basically caused by the opposite sign vortex shed from the soft dorsal fin.
2) The increase in effective AOA leads to LE stall and destabilization of the separated shear layer thus causing the formation of the LE stall vortex as clearly seen in figure 13.
3) The early formation of the vortex in Configuration II results in a decrease in pressure on the suction surface of the tail fin. This increases the pressure differential on the tail fin, which in turn increases the thrust of the tail fin. Details of the pressure forces acting over the pressure and suction sides of tail fin are given in Akhtar[11].
4) The mechanism observed here does not fall into any of the categories proposed by Gopalakrishnan[10].

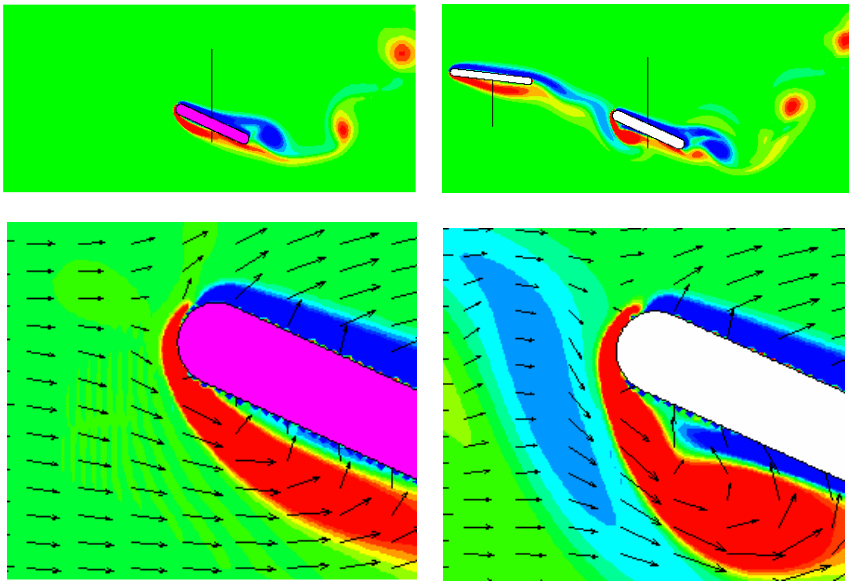

**Figure 13. Comparison and Close up view of Configuration I & II (Note that every 6th vector is plotted in each dimension).**

### C. Phase Difference Study

Analysis of the vortex structures indicates that the physics of thrust enhancement is associated with the interaction of a clockwise rotating vortex with the LE of the tail fin as it moves up (and vice versa). It seems clear that the phase lag between the two fins would be a crucial factor since it will determine the timing of the interaction between the dorsal fin vortices and the tail fin LE. Thus, it seems evident that the examination of the effect of the phase difference between the two fins would lead to further insights into the physics of this flow.

Numerical simulations were carried out assuming different phase differences between fins. With the soft dorsal fin still leading, phase differences of 138°, 123°, 108°, 93°, 78°, 63°, 48°, 33° and 18° were used at the same Reynolds number. Figure 14 shows the vorticity plots for different phase differences when the tail fin is at its mean position with maximum pitch angle. It clearly depicts the effect of phase difference on the vortex structure below the tail fin.

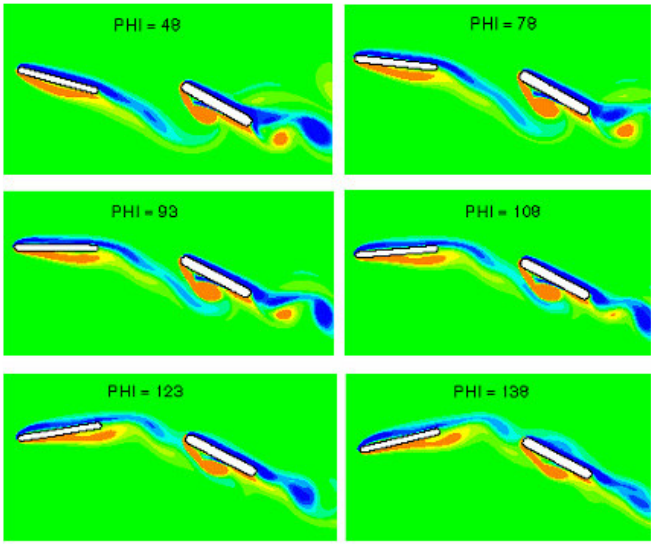


**Figure 14. Vorticity plots for phase difference study**

*1. Effect of Phase Difference on Thrust of Tail Fin*

Figure 15 shows a plot of thrust coefficient of the tail fin versus phase angle. On the right vertical-axis, the thrust on the tail fin (with the dorsal fin upstream) normalized by the thrust of the tail fin (in the absence of the dorsal fin) is plotted. This gives us a direct measure of the tail fin thrust enhancement due to the presence of the dorsal fin.

The encircled value indicates the phase difference of 108°, which was based on the initial experimental value. As found before, the thrust is almost twice that of Configuration I. It is interesting to see that as the phase difference between the soft dorsal and the tail fins is increased to 123°, the thrust starts to decrease but is still greater than for Configuration I. However, as the phase difference is increased further, the thrust decreases to a value lower than that of Configuration I. This clearly implies that the mere presence of a soft dorsal fin upstream is not always beneficial to swimming. Decreasing the phase difference causes the thrust to increase as shown for the cases of 93° and 78°. When the phase difference is 48°, the maximum thrust is achieved, which is just over three times the thrust of the single tail fin case. Decreasing the phase difference further does not increase the thrust.

*2. Effect of Phase Difference on Efficiency of Tail Fin*

Figure 16 shows the variation of efficiency of the tail fin. The phase difference of 108° is encircled where there is a 50% increase in efficiency. As the phase difference is increased, the efficiency goes down, but it remains nearly 30% larger than that of Configuration I. As the phase difference is reduced, the efficiency increases. At a phase difference of 48°, the efficiency is maximum – almost 80% more than that of Configuration I. Increasing the phase difference further, begins to reduce the efficiencies. It is observed that, like thrust, efficiency also peaks at 48°.

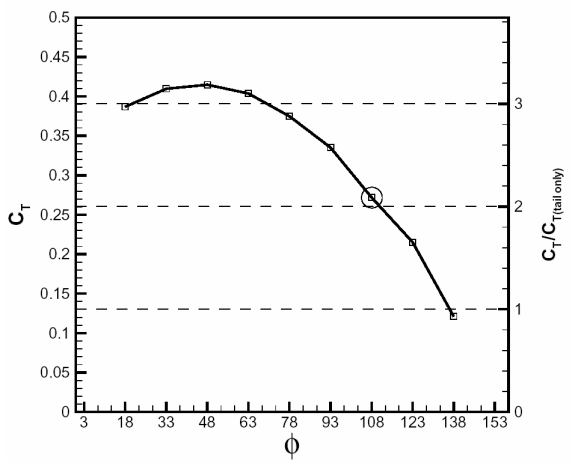


**Figure 15. Thrust coefficient of the tail fin vs Phase difference**

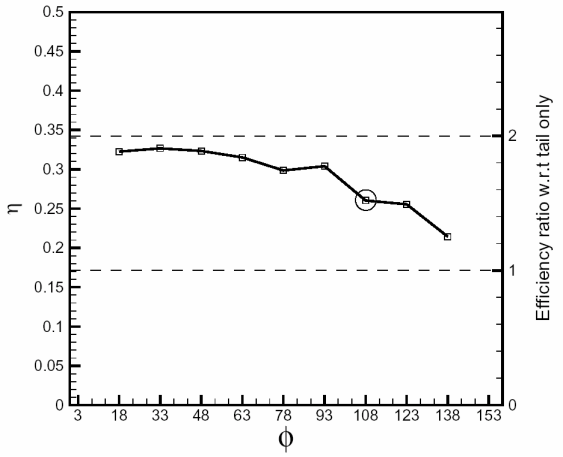


**Figure 16. Efficiency vs Phase difference**

**D. Overall Efficiency of Sunfish**

In the previous sections, the thrust and efficiency of the tail fin have been discussed with or without the presence of upstream dorsal fin. The performance parameters were discussed and compared only for the tail fin. However, in case of the two-fin system, it is logical to calculate these parameters for the whole system and then to compare it to a single fin. This aspect is significant in designing an AUV having a fish-like propulsive system. The comparison presents an analysis of the cost of having a upstream fin. The overall efficiency is calculated by considering the wasted power of the dorsal fin as well. Thus the efficiency of the sunfish can be calculated by the following formula:

$$\eta_p = \frac{(\langle T_{dorsal} \rangle + \langle T_{tail} \rangle) U_\infty}{P_{dorsal} + P_{tail}} \tag{9}$$

Figure 17 shows the comparison of the thrust of the tail fin and the thrust of the tandem fin system. There is a slight decrease in the overall thrust, which is due to the small amount of drag produced by the soft dorsal fin. The reduced thrust is still higher than the thrust of a single tail fin for the phase angle of 108°. Figure 18 shows the comparison of overall efficiency and it follows the same trend but is slightly reduced, as there is a part of wasteful energy being added from the dorsal fin. Still, the efficiency is greater than that of the single fin. This study indicates that the tandem foil system with a suitable phase lag between two fins is better than a single fin.

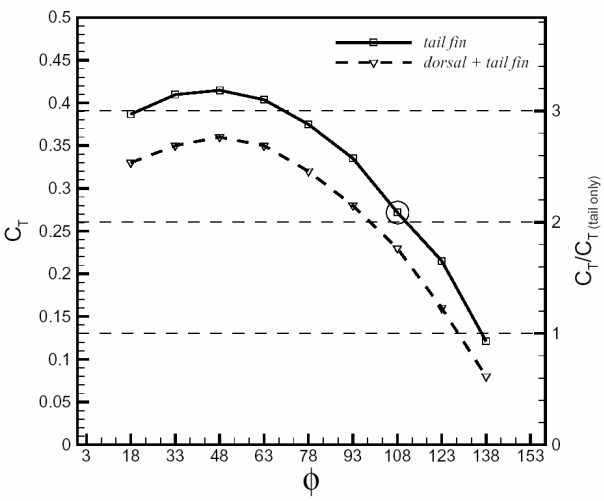


**Figure 17. Thrust vs Phase (Solid line is replotted from Figure 15 for comparison)**

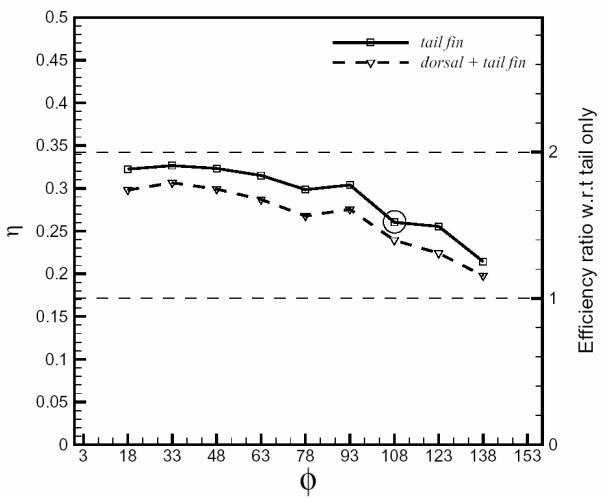


**Figure 18. Efficiency vs Phase (Solid line is replotted from Figure 16 for comparison)**

### E. Wake Topology

We have shown that the presence of the soft dorsal fin causes the shear layer to destabilize and results in early formation of a vortex. It increases thrust and also results in higher efficiency of the tail fin. Figure 15 shows that the phase difference of 48°, produces more thrust than any other phase difference discussed in the study. At the outset, the reason for this is not clear since the size of the LE vortex is about the same for the 48° case as it is for 108° case, observed in figure 19, 20 and 21. Further examination reveals that there is a significant difference in the wake topology for these two cases. For the $\phi$ = 108° case, the wake of the tail fin is dominated by the vortices that are generated by the tail. These vortices are quite widely spaced and do not exhibit any interaction or arrangement. In contrast, for the $\phi$ = 48° case, the wake consists of vortices generated both by the dorsal fin as well as the tail fin. Consequently, the mean spacing between the vortices is lower which leads to significant mutual interaction between the vortices, Interestingly, it is observed that one strong vortex from the tail fin arranges itself in a Karman-like vortex street with two vortices (one from the tail and one from the dorsal fin) which are both rotating counter to the single tail fin vortex. The formation of this street forms a directed jet and consequently increases the thrust on the foil. The same is not the true for the $\phi$ = 138° case since the vortex topology does not orient to produce a strong directed jet.

## V. Conclusion

Two-dimensional numerical simulations have been used to examine the performance of a foil undergoing flapping motion in the wake of another flapping foil. This configuration attempts to mimic the interaction of the dorsal and tail fin observed in a bluegill sunfish by Drucker & Lauder[4-6]. The presence of the upstream flapping foil increases the performance (thrust and efficiency) of the downstream foil by a significant factor. This provides support for the hypothesis of Drucker and Lauder[4-6] that the dorsal fin increases the thrust of the caudal fin though it does not actively participate in the thrust generation. Numerical simulations also allow us to determine the mechanism responsible for this performance enhancement. It is found that vortex structures shed by the upstream fin initiate the formation of a strong leading edge stall vortex on the downstream fin. This stall vortex convects down the surface of the foil and the low pressure associated with this vortex increases the thrust on the downstream foil. The phase lag between the two foils is the key parameter that determines the extent of thrust enhancement. For this particular configuration, the highest performance enhancement is found when the downstream fin motion lags that of the upstream fin by 48°. For this phase angle, it is found that the vortex structures in the composite wake of the two foils arrange themselves in a Karman-like vortex street which is known to be the optimal wake topology for thrust production.

D - Vortex shed by dorsal fin
T - Vortex shed by tail fin

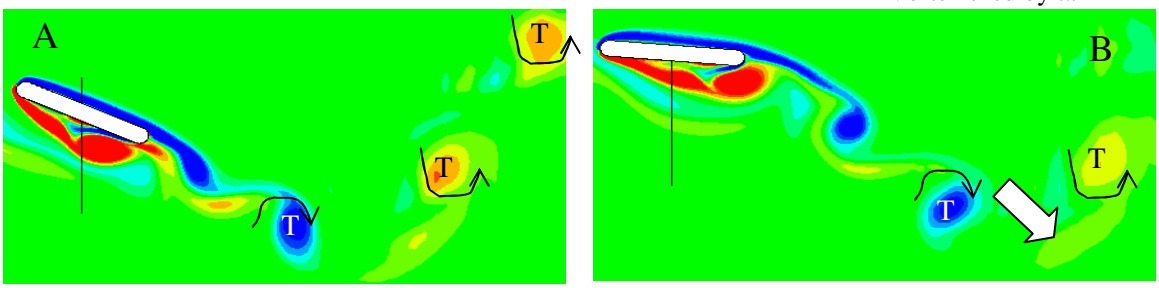


**Figure 19. Close up view of figure 7 (H & K) – 108 deg**

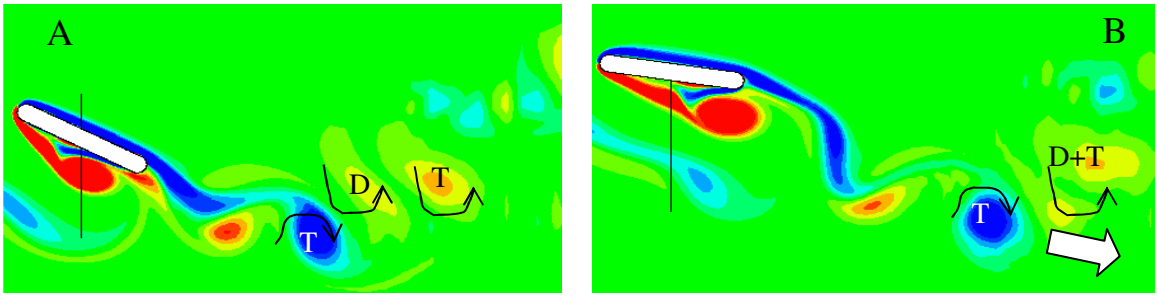


**Figure 20. Close up view for 48 deg phase**

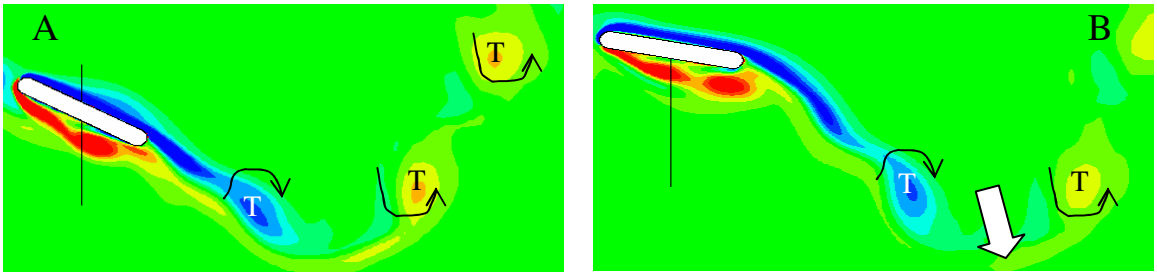


**Figure 21. Close up view for 138 deg phase**


## Acknowledgement

We would like to acknowledge George Lauder and Elliot Drucker for providing the bluegill sunfish data and for extensive discussions. RM would like to acknowledge support from ONR MURI grant N00014-D3-1-0897.


## References


[1]Sfakiotakis, M., Lane, D.M., Davies, J.B.C. 1999. Review of Fish Swimming Modes for Aquatic Locomotion. IEEE *J. Ocean Eng*. Vol. 24(2)

[2]Triantafyllou, G.S., Triantafyllou, M.S., & Grosenbaugh, M.A., 1993. Optimal Thrust Development in Oscillating Foils with Application to Fish Propulsion, *Journal of Fluids and Structures*, 7, 205-224.

[3]Anderson, J.M., Kerrebrock, P.A. 1997. The vorticity control unmanned undersea vehicle (VCUUV) – An autonomous vehicle employing fish swimming propulsion and maneuvering. *Proc. 10th Int. Symp. Unmanned Untethered Submersible Technology*, NH pp.189-195

[4]Drucker, E.G., Lauder, G.V. 1999. Locomotor forces on a swimming fish: three-dimensional vortex wake dynamics quantified using digital particle image velocimetry. *J. Exp. Bio.* 202: 2393-2412.

[5]Drucker, E.G., Lauder, G.V. 2000. A hydrodynamic analysis of fish swimming speed: wake structure and locomotor force in slow and fast labriform swimmers. *J. Exp. Bio.* 203:2379-2393

[6]Drucker, E.G., Lauder, G.V. 2001. Locomotor function of the dorsal fin in teleost fishes: experimental analysis of wake forces in sunfish. *J. Exp. Bio*. 204:2943-58

[7]Udaykumar, H.S., Mittal, R. and Shyy, W. 1999. Computation of solid liquid phase fronts in the sharp interface limit on fixed grids. *J. Comp. Phys.*, 153, 535.

[8]Ye, T., Mittal, R.,UdayKumar, H.S. and Shyy, W. 1999. An accurate cartesian grid method for viscous incompressible flows with complex immersed boundaries, *J. Comp. Phys*. Vol 156, pp 209-240.

[9]Triantafyllou, G.S., & Triantafyllou, M.S., Streitlien, K., 1996. Efficient Foil Propulsion through Vortex Control, AIAA *Journal*, 34 (11), pp 2315-2319.

[10]Gopalkrishnan, R., Triantafyllou, M.S., Triantafyllou, G.S. & Barrett, D.S. 1994. Active Vorticity Control in a Shear Flow Using a Flapping Foil. *Journal of Fluid Mechanics*, 274, 1-21.

[11]Akhtar, I., "Thrust Augmentation through Active Flow Control –Lesson from Bluegill Sunfish", MS Thesis, The George Washington University, 2003.